JOURNAL OF MATERIALS SCIENCE 21 (1986) 1020–1026

Tensile strength and flux pinning force of superconducting Nb_3Sn compound as a function of grain size

SHOJIRO OCHIAI, TOSHIHIRO UEHARA, KOZO OSAMURA
Department of Metallurgy, Kyoto University, Sakyo-ku, Kyoto 606, Japan

In order to evaluate the influence of grain size on the strength and flux pinning force of the Nb_3Sn compound, the microstructure, tensile behaviour and flux pinning force of the bronze-processed Nb_3Sn superconducting composite materials were investigated under various heat treatments. It was found that the strength of the Nb_3Sn layer has a strong dependency on the grain size and it can be expressed by the Hall–Petch type relation. The flux pinning force was roughly proportional to the inverse grain size, agreeing with the results of former investigations.

1. Introduction

As the superconducting Nb_3Sn compound is brittle, it fractures at low strain. This not only has serious consequences for handling but also gives a limit of strain tolerance in superconducting properties [1–4]. Thus it is very important to know the fracture behaviour and strength of the Nb_3Sn compound. Although the deformation and fracture behaviour of the Nb_3Sn layer in composites has been studied in detail [5, 6], the strength of this layer has not been clarified up to date.

In the Nb_3Sn superconducting materials, grain boundaries plays important roles. For instance, it is believed that grain boundaries are the primary pinning centres and the flux pinning force increases with decreasing grain size when the grain size is larger than a critical value [7–9]. From the view of fracture behaviour of Nb_3Sn, fracture occurs at the grain boudary. Therefore it is expected that the strength of this compound has a strong dependency on the grain size. The aim of the present work is to measure the tensile strength and flux pinning force of the Nb_3Sn layer in bronze-processed multi-filamentary composites and to obtain the relations of these properties to grain size.

2. Experimental procedure

The specimens employed in the present study were multi-filamentary composites supplied as the Japanese Standard Reference Sample for the superconducting materials group for energy research in 1983 to 1985 of the Ministry of Education, Science and Culture of Japan. The composite specimens were composed of 745 niobium filaments in a Cu–13 wt % Sn alloy, surrounded with a niobium barrier and then pure copper as a stabilizer. The bronze and copper to non-copper ratios were 2 and 0.445, respectively. The diameter of the niobium filaments, d_f, and the thickness of the niobium barrier were, on average, 5.0 and 7.1 μm, respectively.

In order to change the grain size and thickness of the Nb_3Sn layer, two kinds of heat treatment were carried out. For the first heat treatment (HT1), the specimens were annealed isothermally, at 973 and 1073 K up to 4320 ksec, and for the second heat-treatment (HT2), the specimens were annealed at 973, 1023 and 1073 K for 432 ksec. Some of the specimens annealed at 973 K for 432 ksec, which had a very low tin concentration in the Cu–Sn matrix (about 0.2 at %) and therefore would not melt at least below 1300 K [10], were annealed again at 1123, 1173, 1223 and 1273 K for 86.4 ksec. After annealing, each specimen was embedded in resin and then the cross-section was polished. Using this polished cross-section, the thickness of the Nb_3Sn layer, c, the volume fraction of the Nb_3Sn layer, V_{Nb_3Sn}, which is the sum of the volume fractions of the Nb_3Sn layer formed on the niobium filaments and at the niobium barrier, the volume fraction of niobium, V_{Nb}, which is the sum of the volume fractions of the niobium filaments and the niobium barrier remaining after reaction, and tin concentration in the Cu–Sn matrix, x_{Sn}, in which the ZAF correction was carried out, were measured with scanning electron microscopy (SEM) and electron probe microanalysis (EPMA). The volume fraction of copper was 0.308, being unvaried in any heat treatment. The volume fraction of the Cu–Sn matrix was obtained by the equation of $1 - V_{Nb_3Sn} - V_{Nb} - V_{Cu}$.

Tensile tests were carried out with an Instron-type tensile machine at room temperature at a strain rate of $3.33 \times 10^{-3}\,sec^{-1}$. For each annealing treatment, two specimens were tested and the results were averaged. From the fracture surface of the Nb_3Sn layer, the grain size was measured with the linear line intercept method [7].

The critical current was measured in the magnetic field B from 2 to 8 tesla at 4.2 K by a 1 μV criterion for critical current. The critical current density J_c was calculated by dividing the critical current by the real cross-sectional area of the Nb_3Sn layer itself. The flux pinning force F_p (which equals J_cB) was plotted against B and the maximum value of F_p, $F_{p,max}$, was obtained.

0022–2461/86 $03.00 + .12

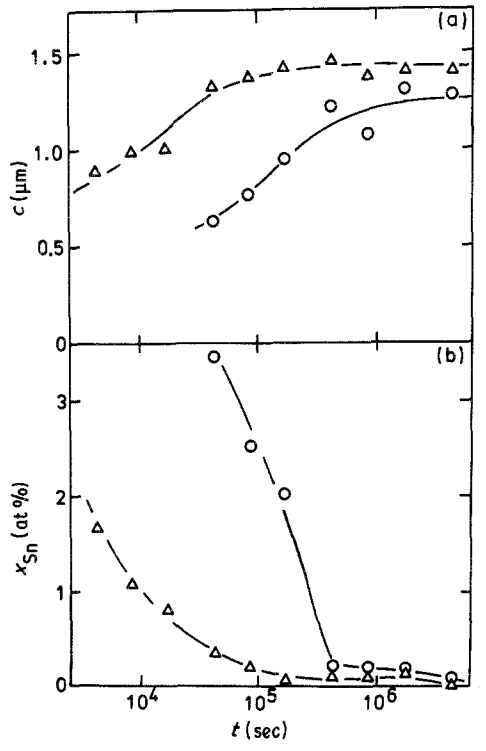

Figure 1 Variations of (a) c and (b) x_{Sn} fo the specimens annealed as a function of t. ○: 973 K; △: 1073 K.

3. Results and discussion

3.1. Microstructure of the composites

The thickness of the Nb_3Sn layer, c, increased and correspondingly, the tin concentration in the Cu–Sn matrix, x_{Sn}, decreased with increasing annealing time under HT1 treatment, as shown in Fig. 1. Fig. 2 shows the variation of c as a function of final annealing temperature T, below 1073 K the specimens were annealed for 432 ksec, and above 1123 K they were annealed for 86.4 ksec after having been annealed at 973 K for 432 ksec (HT2). c increased with increasing T. x_{Sn} in these specimens were less than 0.2 at %. The variations of V_{Nb_3Sn} and V_{Nb} for HT1 and HT2 treatments are shown in Figs. 3 and 4, respectively. V_{Nb_3Sn} increased and correspondingly V_{Nb} decreased with at increasing annealing time and final annealing temperature.

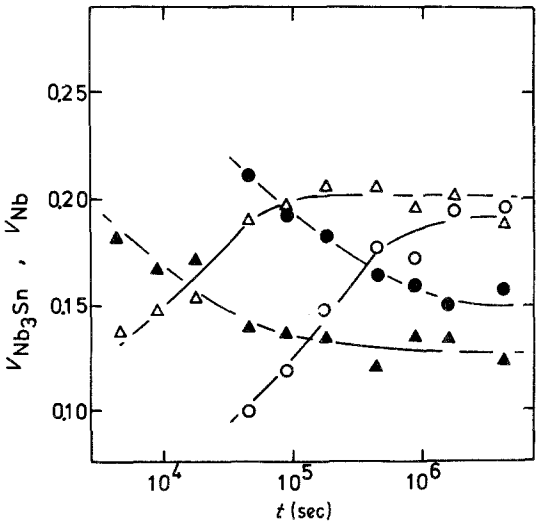

Figure 3 Variations of V_{Nb_3Sn} and V_{Nb} of the specimens annealed as a function of t. ○: V_{Nb_3Sn}, 973 K; ●: V_{Nb}, 973 K; △: V_{Nb_3Sn}, 1073 K; ▲: V_{Nb}, 1073 K.

Fig. 5 shows typical fracture surfaces of the Nb_3Sn layer after annealing at (a) 973 K for 432 ksec, (b) 1073 K for 432 ksec, (c) 1173 K for 86.4 ksec after having been annealed at 973 K for 432 ksec and (d) 1273 K for 86.4 ksec after having been annealed at 973 K for 432 ksec. It is evident that the grain size increased with increasing final annealing temperature. The shape of the grain was columnar near the Nb–Nb_3Sn interface but rather equiaxed near the Nb_3Sn–(Cu–Sn) interface at annealing temperatures of 973 and 1073 K. The columnar grain dimensions in the growth direction were about 2 to 4 times (973K) and about 1 to 2 times (1073K) larger than those transverse to the grain direction. Such dimension ratio values has been reported also for V_3Ga [11]. On the other hand, above 1123 K, the grain became nearly equiaxed and of cubic symmetry. From the photographs as shown in Fig. 5, the average grain size d after HT2 treatment was measured with the line intercept method as shown in Fig. 6. For the columnar grains, this method was applied in both directions of grain growth and perpendicular to it, and the results

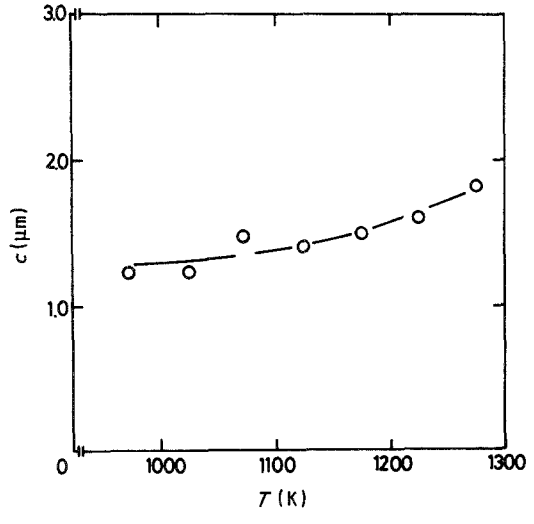

Figure 2 Variation of c of the specimens after HT2 treatment as a function of final annealing temperature.

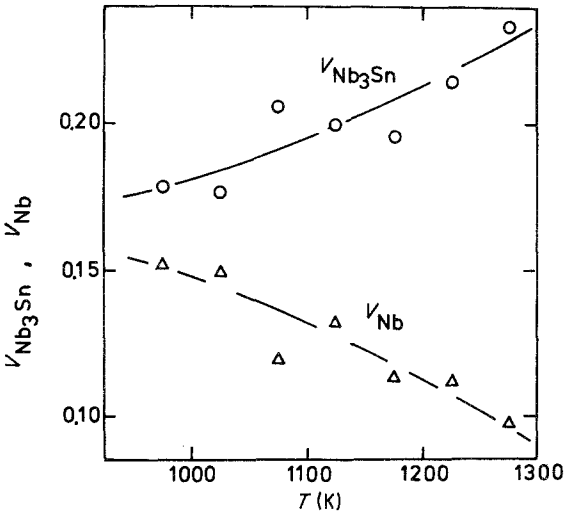

Figure 4 Variations of V_{Nb_3Sn} and V_{Nb} of the specimens after HT2 treatment as a function of final annealing temperature.

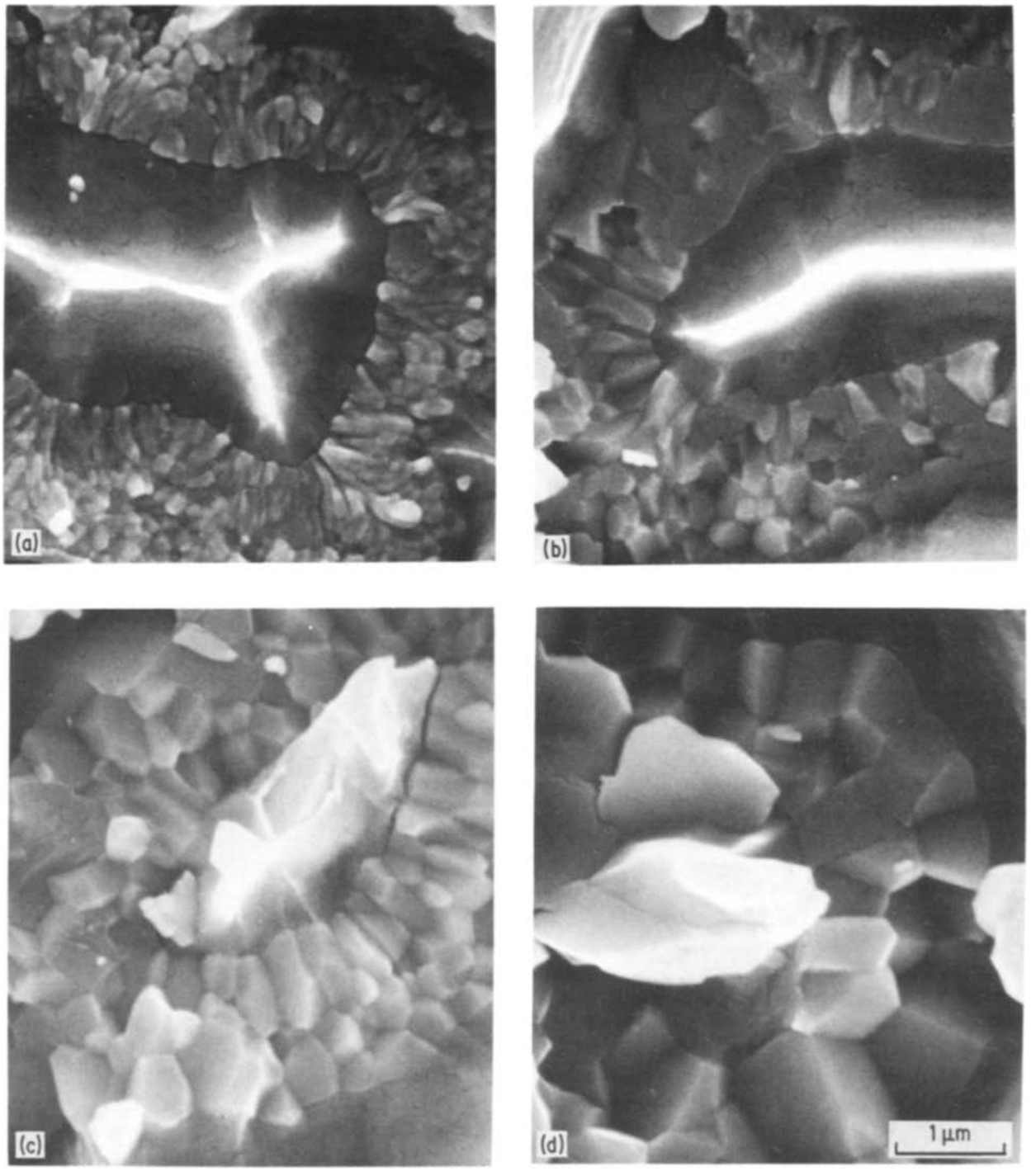

Figure 5 Fracture surfaces of the Nb_3Sn layer in the specimens annealed (a) at 973 K for 432 ksec, (b) at 1073 K for 432 ksec, (c) at 1173 K for 86.4 ksec after annealing at 973 K for 432 ksec and (d) at 1273 K for 86.4 ksec after annealing at 973 K for 432 ksec.

were averaged. Similarly, the variation of the average grain size of the Nb_3Sn layer after HT1 treatment was measured as shown in Fig. 7. It is evident that the grain size increased with increasing annealing time at both annealing temperatures of 973 and 1073 K, as has been observed by Scanlan *et al.* [7].

3.2. Flux pinning force as a function of grain size

The critical current measurements were carried out for the four different grain sizes; 0.20 μm (heat treatment at 973 K for 432 ksec), 0.24 μm (973 K, 1730 ksec), 0.32 μm (1023 K, 432 ksec) and 0.44 μm (1073 K, 432 ksec). The measured values of the flux pinning force F_p are shown in Fig. 8 as a function of applied magnetic field B. The pinning force is influenced by many factors such as grain size, grain shape and stoichiometry of the Nb_3Sn layer and also residual stresses arising from the difference in thermal contractions among the constituents. Among these factors, the increase in the pinning force with decreasing grain size has been predicted in various theories on flux pinning by grain boundaries [12–14]. Especially, at least within the range of grain size smaller than about 0.1 μm, it has been demonstrated by many investigators [7–9, 15] that the flux pinning force is roughly proportional to the inverse grain size. The present result agreed with these investigations, although the

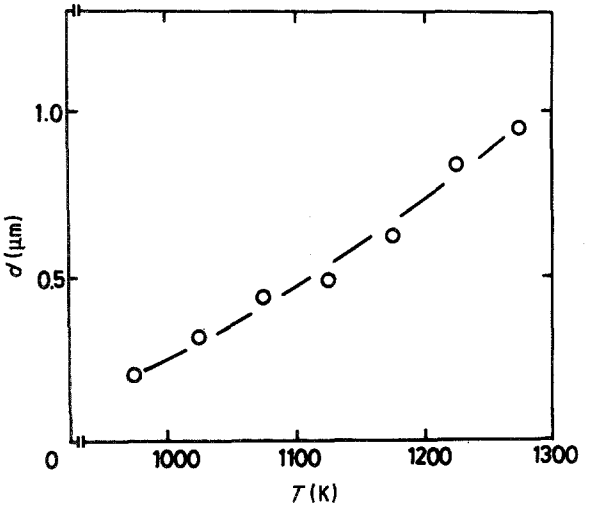

Figure 6 Average measured values of d after HT2 treatment as a function of final annealing temperature.

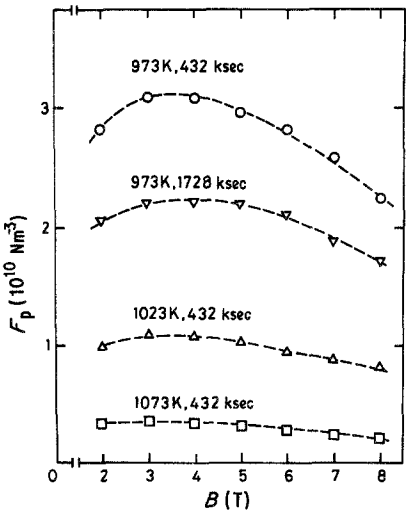

Figure 8 Measured values of F_p plotted against B.

aforementioned factors other than grain size might affect the pinning force to some extent, as shown in Fig. 9 where the maximum pinning force, $F_{p,max}$, which was read from the F_p–B curves shown in Fig. 8, is plotted against the inverse grain size.

3.3. Tensile behaviour of composites

Fig. 10 shows typical stress–strain curves of the composite specimens annealed at 973 K for 43.2, 173 and 432 ksec. The specimens annealed for 43.2 and 173 ksec showed large plastic deformation, while the specimen annealed for 432 ksec fractured in a brittle manner without apparent plastic deformation. These two types of fracture mode of bronze-processed Nb_3Sn superconducting materials have been observed and analysed in our following work [6]. As in our following work, the fracture mode of the former specimens are named as type I and that of the latter as type II. Within the range investigated in the present work, only the specimens annealed at 973 K for 43.2, 86.4 and 173 ksec and that annealed at 1073 K for 4.43 ksec showed type I but the other specimens showed type II; namely type I mode occurred in the specimens with low V_{Nb_3Sn} and type II in the specimens with high V_{Nb_3Sn}. The reason, why the specimens with low V_{Nb_3Sn} showed type I but those with high V_{Nb_3Sn} type II, could be attributed to the difference in the load bearing capacity of composites due to breakage of the Nb_3Sn layer that can be compensated by the work hardening of the ductile constituents of copper, Cu–Sn and niobium when V_{Nb_3Sn} is low but not when it is high, as demonstrated [6] using the theory of fibre reinforcement [16–18].

In order to know when the Nb_3Sn layer begins fracturing in composites, the appearance of the Nb_3Sn layer after loading to various strain levels was examined with the SEM by etching away the copper, the niobium barrier and some portion of the Cu–Sn matrix. It was found that, in the specimens which showed type I mode, the Nb_3Sn layer begins fracturing when apparent plastic deformation of composites as a whole takes place. Fig. 11 shows an example of the appearance of the Nb_3Sn layer at various strains shown in the stress–strain curves. In this example, taken from the specimen annealed at 973 K for 43.2 ksec, fracture of Nb_3Sn layer has started at the strain ② in the stress–strain curve, which is just after the initiation of apparent plastic deformation. Not only in this example but also in all specimens showing type I mode, the

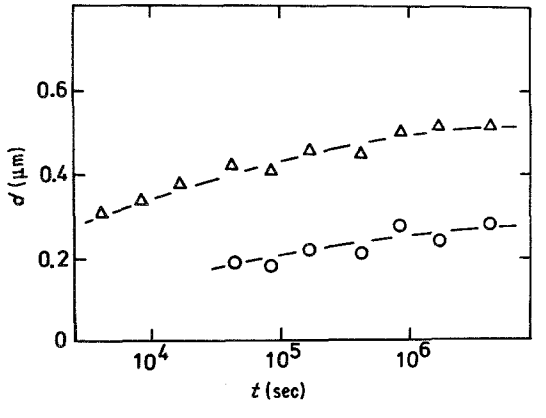

Figure 7 Average measured values of d of the specimens annealed as a function of t. ○: 973 K; △: 1073 K.

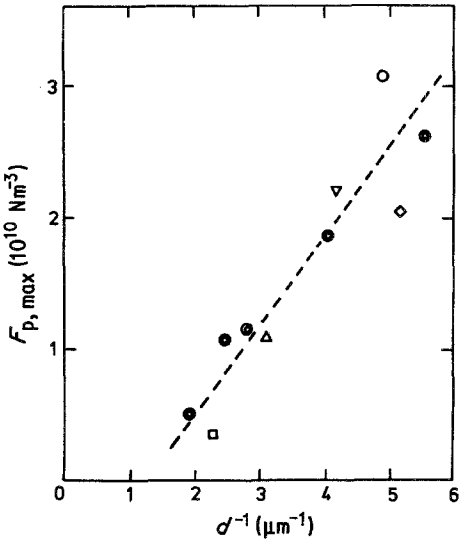

Figure 9 Measured values of $F_{p,max}$ plotted against $1/d$. ○: 973 K, 432 ksec; ▽: 973 K, 1730 ksec; △: 1023 K, 432 ksec; ⊙: Scalan *et al.* [7]; ◇: Livingston (B = 4T) [8].

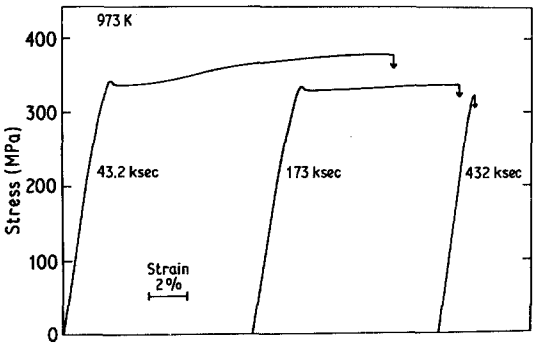

Figure 10 Typical stress–strain curves of the specimens annealed at 973 K for various times.

Nb_3Sn layer was broken into shorter and shorter lengths with increasing strain after the start of fracturing, showing multiple fracture at high strains as shown in Fig. 11. On the other hand, in the specimens which showed type II mode, it was found that most of the Nb_3Sn layer fractured at the fracture of composites as a whole while only a small number of fractures of the Nb_3Sn layer occurred prior to the fracture of composites as a whole. Therefore, in type II specimens, the fracture strain of the Nb_3Sn layer is approximately equal to that of composites as a whole.

3.4. Tensile strength of the Nb_3Sn layer

The multiple fracture phenomenon of the Nb_3Sn layer can occur only when the V_{NB_3Sn} is low and the drop of load-bearing capactity of composites due to breakage of the Nb_3Sn layer can be compensated by the work hardening of ductile constituents [6, 16, 17]. On the other hand, when V_{Nb_3Sn} is high, as the drop of the load-bearing capacity cannot be compensated by the work hardening of the ductile constituents, the fracture of the Nb_3Sn layer causes fracture of the composite as a whole. Therefore the stress at which multiple fracture of the Nb_3Sn layer starts occurring in type I and the stress at fracture of composites in type II could be regarded as the stress at which the Nb_3Sn layer shows its strength, to a first approximation. Noting the composite stress at which the Nb_3Sn layer shows its strength as σ_c^A, σ_c^A is approximately given by

$$\sigma_c^A = \sigma_{Nb_3Sn} V_{Nb_3Sn} + \sigma^*_{Cu} V_{Cu} + \sigma^*_{Cu\text{–}Sn} V_{Cu\text{–}Sn} + \sigma^*_{Nb} V_{Nb} \quad (1)$$

from the rule of mixtures [6, 16, 19] where σ_{Nb_3Sn} is the tensile strength of the Nb_3Sn layer and the σ^*_{Cu}, $\sigma^*_{Cu\text{–}Sn}$ and σ^*_{Nb} are the stresses of copper, Cu–Sn and niobium at the fracture strain of the Nb_3Sn layer. σ_{Nb_3Sn} can be evaluated by substituting the measured values of σ_c^A, V_{Nb_3Sn}, V_{Cu} and $V_{Cu\text{–}Sn}$, and the values of $\sigma^*_{Cu\text{–}Sn}$, σ^*_{Cu} and σ^*_{Nb} into Equation 1. As the fracture strain of the Nb_3Sn layer is very low compared with that of Cu–Sn and copper, the $\sigma^*_{Cu\text{–}Sn}$ and σ^*_{Cu} can approximately be given by respective yield stress [6]. Using the data of the yield stresses of annealed Cu–Sn alloy for various tin concentrations [20], the yield stress of this alloy, $\sigma_{Cu\text{–}Sn,y}$, was expressed as a function of tin concentration in the form given by

$$\sigma_{Cu\text{–}Sn,y} = 70 + 22\,x(\text{at \% Sn}) \quad \text{MPa} \quad (2)$$

Substituting the measured values of tin concentration, x_{Sn}, into Equation 2, the value of $\sigma^*_{Cu\text{–}Sn}$ was obtained in each specimen. For σ^*_{Cu}, the value of $\sigma_{Cu\text{–}Sn,y}$ at $x_{Sn} = 0$, 70 MPa was used. As the yield stresses of the niobium filaments and the niobium barrier could not be measured separately, it was assumed that both of the niobium filaments and the niobium barrier show the same yield stress under a given annealing treatment. The yield stress of niobium was measured by using the niobium filaments with a diameter of 0.65 mm supplied by Sumitomo Electric Industries Ltd, Japan, after the respective annealing treatment. It was found that the time dependency of the yield stress of niobium at annealing temperatures of 973 and 1073 K is small. Therefore the average values of the yield stress, 233 MPa at 973 K annealing and 210 MPa

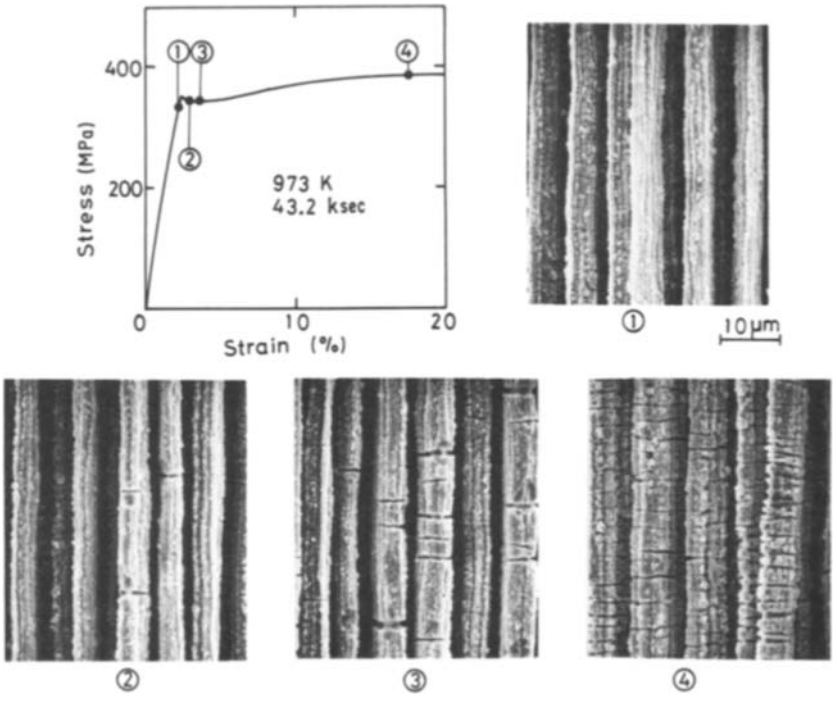

Figure 11 Appearance of the Nb_3Sn layer at the strains indicated in the stress–strain curve of the specimen annealed at 973 K for 43.2 ksec, which showed type I fracture mode.

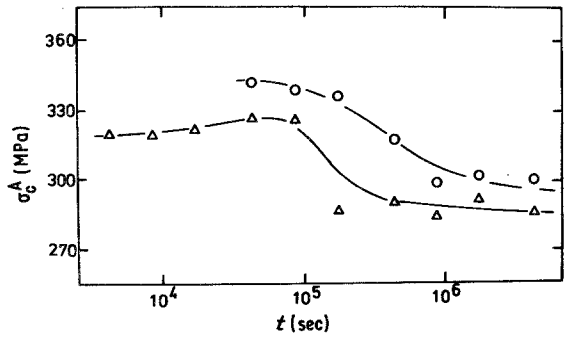

Figure 12 Variations of σ_c^A as a function of t of the specimens annealed isothermally. ○: 973 K; △: 1073 K.

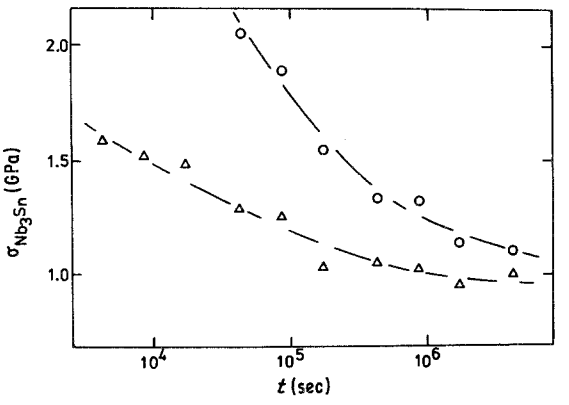

Figure 14 Variation of σ_{Nb_3Sn} as a function of t of the specimens annealed isothermally. ○: 973 K; △: 1073 K.

at 1073 K annealing, were used as σ_{Nb}^*. Under HT2 treatment, the yield stress of the niobium filaments had little dependency on final annealing temperature above 1123 K, being nearly constant at 210 MPa. This value of 210 MPa was used as σ_{Nb}^* for the final annealing temperature above 1123 K. This value is nearly the same as the reported value of the yield stress of the fully annealed wrought niobium, 207 MPa [21].

In composite specimens annealed to form Nb_3Sn layers and then cooled to room temperature, the Nb_3Sn layer, niobium filaments and barrier are subjected to compressive residual stresses and the copper and Cu–Sn to tensile residual stresses [22]. When the composites are pulled in tension, the stress exerted on the Nb_3Sn layer increases from minus to zero and then becomes plus with increasing applied tensile stress. As the σ_c^A corresponds to the stress at which the Nb_3Sn layer fractures in tension, the estimated values of σ_{Nb_3Sn} show the tensile strength [6].

Figs. 12 and 13 show the measured values of σ_c^A for HT1 and HT2 treatments, respectively. From the measured values of σ_c^A shown in Figs. 12 and 13, the σ_{Nb_3Sn} was calculated as shown in Figs. 14 and 15, respectively. It is evident that the longer the annealing time and the higher the annealing temperature, the lower becomes the σ_{Nb_3Sn}. As shown already the grain size increased with increasing annealing time and temperature. Then all values of the σ_{Nb_3Sn} shown in Figs. 14 and 15 were plotted against grain size d to check the dependency of the strength on the grain size. Fig. 16 shows the result. It is clear that the larger the grain size, the lower the strength.

Efforts were made to find a relation of σ_{Nb_3Sn} to d. It was found that σ_{Nb_3Sn}, to a first approximation, is proportional to $d^{-1/2}$ as shown in Fig. 17. This type of the relation is known as the Hall–Petch relation [23, 24]. This relation has been derived on the basis of the mechanism that a crack is nucleated by a dislocation pile-up process against grain boundaries and therefore microscopic plastic flow is the cause of fracture [23–25]. In this mechanism, plastic deformation or dislocation movement is inevitable. At present, it is, however, unknown whether plastic deformation occurs or not in the Nb_3Sn compound when pulled in tension at room temperature, although it has been confirmed that plastic flow occurs under high hydrostatic pressure even at room temperature and also under no and ambient pressure at elevated temperatures [26–28]. Therefore it cannot be concluded that the strength of the Nb_3Sn compound obeys the Hall–Petch relation in a rigid manner. Although the reason, why the Hall–Petch type relation can describe the strength of Nb_3Sn layer, is not known at present, this type of the relation can be employed at least as an empirical one to describe the strength as a function of grain size. This is the first finding for the Nb_3Sn compound.

4. Conclusions

The tensile strength and flux pinning force of the Nb_3Sn layer were expressed as a function of grain size, to a first approximation. The flux pinning force was proportional to the inverse grain size as in the former

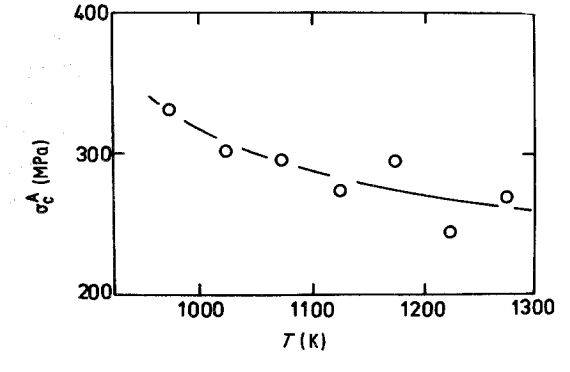

Figure 13 Variations of σ_c^A as a function of final annealing temperature of the specimens after HT2 treatment.

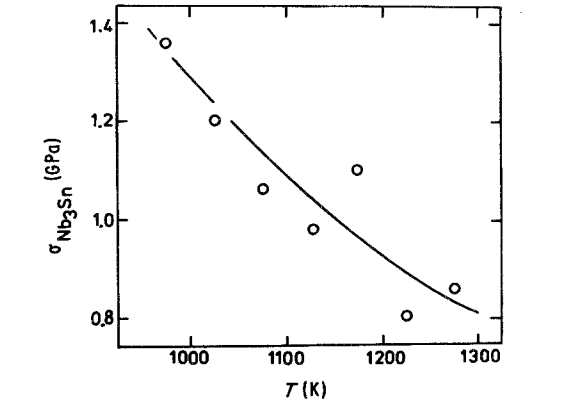

Figure 15 Variations of σ_{Nb_3Sn} as a function of final annealing temperature of the specimens after HT2 treatment.

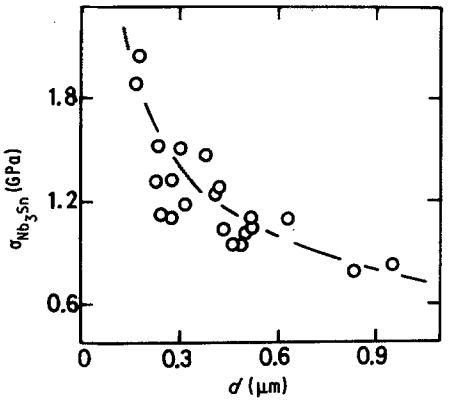

Figure 16 Decrease in σ_{Nb_3Sn} with increasing d.

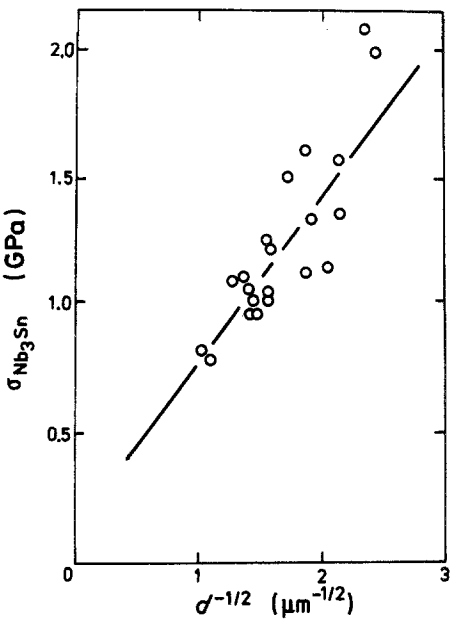

Figure 17 σ_{Nb_3Sn} plotted against $d^{-1/2}$.

investigations and the strength was described by the Hall–Petch type relation empirically.

Acknowledgements

The authors wish to express their gratitude to Messrs T. Unesaki and I. Nakagawa at Kyoto University for their help in the SEM and EPMA studies, and to Messrs M. Nagata and S. Okuda at Sumitomo Electric Industries Ltd, Osaka, Japan, for their help in measuring the critical current at 4.2 K. They also express their gratitude to the Ministry of Education, Science and Culture of Japan for the grand-in-aid for energy research (No. 60 055 023).

References

1. J. W. EKIN, in "Superconducting Materials Science-Metallurgy, Fabrication and Applications", edited by S. Foner and B. B. Schwartz (Plenum Press, New York, 1981) p. 455.
2. T. LUHMAN, M. SUENAGA, D. O. WELCH and K. KAIHO, *IEEE Trans. Mag.* **MAG-15** (1979) 699.
3. G. RUPP, in "Filamentary A15 Superconductors", edited by M. Suenaga and A. F. Clark (Plenum Press, New York, 1980) p. 155.
4. T. LUHMAN and D. O. WELCH, *ibid.* p. 171.
5. I. PHEIFFER and E. SPRINGER, *Z. Metallkde.* **68** (1977) 667.
6. S. OCHIAI, K. OSAMURA and T. UEHARA, *J. Mater. Sci.* **21** (1986) 1027.
7. R. M. SCANLAN, W. A. FIETZ and E. F. KOCH, *J. Appl. Phys.* **46** (1975) 2244.
8. J. D. LIVINGSTON, *Phys. Status Solidi* **44** (1977) 295.
9. W. SCHAUER and W. SCHELB, *IEEE Trans. Mag.* **MAG-17** (1981) 374.
10. M. HANSEN, in "Constitution of Binary Alloys" (McGraw-Hill, New York, 1958) p. 633.
11. Y. TANAKA, K. ITO and K. TACHIKAWA, *J. Jpn. Inst. Met.* **40** (1976) 514.
12. A. M. CAMBELL and J. E. EVETTS, *Adv. Phys.* **21** (1972) 199.
13. E. J. KRAMER and G. S. KNAPP, *J. Appl. Phys.* **46** (1975) 4595.
14. C. S. PANDE and M. SUENAGA, *Appl. Phys. Lett.* **29** (1976) 443.
15. B. J. SHAW, *J. Appl. Phys.* **47** (1976) 2143.
16. A. KELLY and W. R. TYSON, *J. Mech. Phys. Solids* **13** (1965) 329.
17. S. OCHIAI, M. MIZUHARA, K. SHIMOMURA and Y. MURAKAMI, *Trans. Jpn. Inst. Met.* **16** (1975) 345.
18. S. OCHIAI and K. OSAMURA, *Z. Metallkde.* **76** (1985) 485.
19. D. L. McDANELS, R. W. JECH and J. W. WEETON, *Trans. Met. Soc. AIME,* **233** (1965) 636.
20. ASM Committee on Copper and Copper Alloys, Metals Handbook, "Properties and Selections: Nonferrous Alloys and Pure Metals" Vol. 2 (ASM, Metals Park, Ohio, 1979) p. 275.
21. G. T. MURRAY, *ibid.* p. 709.
22. D. S. EASTON, D. M. KROEGER, W. SPECKING and C. C. KOCH, *J. Appl. Phys.* **51** (1980) 2748.
23. E. O. HALL, *Proc. Phys. Soc.* **64B** (1951) 747.
24. N. J. PETCH, *J. Iron Steel Inst.* **173** (1953) 25.
25. A. J. STROH, *Adv. Phys.* **6** (1957) 418.
26. R. N. WRIGHT, *Met. Trans.* **8A** (1977) 2024.
27. L. R. EISENSTATT and R. N. WRIGHT, *ibid.* **11A** (1980) 131.
28. J. B. CLARK and R. N. WRIGHT, *ibid.* **14A** (1983) 2295.

Received 19 April
and accepted 31 May 1985